RSC Advances

PAPER

View Article Online
View Journal | View Issue

Open Access Article. Published on 02 February 2016. Downloaded on 12/4/2025 4:25:01 PM.
This article is licensed under a Creative Commons Attribution 3.0 Unported Licence.

Cite this: *RSC Adv.*, 2016, **6**, 16150

Dye-sensitized solar cell based on an inclusion complex of a cyclic porphyrin dimer bearing four 4-pyridyl groups and fullerene C_{60}†

Yousuke Ooyama,*[a] Koji Uenaka,[a] Takuya Kamimura,[b] Shuwa Ozako,[b] Masahiro Kanda,[a] Taro Koide[b] and Fumito Tani*[b]

Received 14th January 2016
Accepted 1st February 2016

DOI: 10.1039/c6ra01131d

www.rsc.org/advances

Cyclic free-base porphyrin dimers (**H_4-C_4-CPD_{Py}(TEO)** and **H_4-Ptz-CPD_{Py}(TEO)**) linked by butadiyne or phenothiazine bearing four 4-pyridyl groups and their inclusion complexes (**$C_{60}\subset H_4$-C_4-CPD_{Py}(TEO)** and **$C_{60}\subset H_4$-Ptz-CPD_{Py}(TEO)**) with fullerene C_{60} have been applied to dye-sensitized solar cells (DSSCs) as a new class of porphyrin dye sensitizers with pyridyl anchoring groups for attachment on a TiO_2 electrode. The FTIR spectra of the porphyrin dimers adsorbed on TiO_2 nanoparticles demonstrated that these porphyrin dimers are adsorbed on the TiO_2 surface through the formation of hydrogen bonding of pyridyl groups and/or pyridinium ions at Brønsted acid sites on the TiO_2 surface. The adsorption amount of the porphyrin dimers adsorbed on the TiO_2 electrode is 2.0×10^{17} molecules per cm^2, that is, the adsorption amount of the porphyrin unit is 4.0×10^{17} cm^{-2}, which is higher than that of dye sensitizers with pyridyl groups reported so far. The photovoltaic performance of DSSCs based on phenothiazine-bridged cyclic porphyrin dimer **H_4-Ptz-CPD_{Py}(TEO)** is higher than that of DSSCs based on butadiyne-linked cyclic porphyrin dimer **H_4-C_4-CPD_{Py}(TEO)**. Moreover, the photovoltaic performances of DSSCs based on cyclic free-base porphyrin dimers are higher than those of DSSCs based on their C_{60} inclusion complexes **$C_{60}\subset H_4$-C_4-CPD_{Py}(TEO)** and **$C_{60}\subset H_4$-Ptz-CPD_{Py}(TEO)**. On the basis of the electrochemical measurements (voltammetry and electrochemical impedance spectroscopy) and the transient absorption spectroscopy, the differences in the photovoltaic performances among these cyclic free-base porphyrin dimers are discussed from kinetic and thermodynamic considerations concerning the electron transfer processes in DSSCs.

Introduction

Dye-sensitized solar cells (DSSCs) employing dye-adsorbed TiO_2 electrodes are one of the most promising new renewable photovoltaic cells utilizing the sun as a free and inexhaustible energy source because of their interesting construction and operational principles, and low cost of production, since Grätzel and co-workers produced high-performance DSSCs based on a Ru-complex dye, which showed a solar energy-to-electricity conversion yield (η) of 11%.[1] To further improve the photovoltaic performance of DSSCs, many kinds of ruthenium (Ru) dyes, porphyrin dyes, phthalocyanine dyes and organic dyes bearing carboxyl groups as anchoring groups, which are adsorbed on the TiO_2 electrode through the bidentate bridging linkage between the carboxyl group of the dye and Brønsted acid sites (surface-bound hydroxyl groups, Ti-OH) on the TiO_2 surface, have been developed as dye sensitizers during the last two decades.[2–9] In particular, porphyrin dyes have been regarded as promising candidates for photosensitizers as a result of their strong Soret (400–500 nm) and moderate Q band (500–700 nm) absorption properties, as well as their electrochemical, photochemical and thermal stabilities. Much effort in molecular design and development of porphyrin dye sensitizers having carboxyl group have been made to further improve the photovoltaic performances of DSSCs so far.[10–15] Consequently, DSSCs based on donor–π–acceptor (D–π–A) porphyrin dyes bearing the diarylamino group as an electron donor and the benzothiadiazole-benzoic acid moiety as an electron acceptor, which exhibited good absorption features (bathochromic shift and broadening of the Soret and Q bands), have achieved η value of up to *ca.* 13%.[11d,e]

On the other hand, we have reported that a new type of D–π–A dye sensitizers bearing pyridyl group as electron-withdrawing anchoring group were predominantly adsorbed on the TiO_2 electrode through coordinate bonding between the pyridyl

[a]*Department of Applied Chemistry, Graduate School of Engineering, Hiroshima University, Higashi-Hiroshima 739-8527, Japan. E-mail: yooyama@hiroshima-u.ac.jp; Fax: +81-82-424-5494*

[b]*Institute for Materials Chemistry and Engineering, Kyushu University, 744 Motooka, Nishi-ku, Fukuoka 819-0395, Japan. E-mail: tanif@ms.ifoc.kyushu-u.ac.jp; Fax: +81-92-802-6224*

† Electronic supplementary information (ESI) available: ^{1}H NMR and ^{13}C NMR for compounds **1**, **2** and **H_4-C_4-CPD_{Py}(TEO)**. See DOI: 10.1039/c6ra01131d

This journal is © The Royal Society of Chemistry 2016

Open Access Article. Published on 02 February 2016. Downloaded on 12/4/2025 4:25:01 PM.
This article is licensed under a Creative Commons Attribution 3.0 Unported Licence.

group of the dye and the Lewis acid site (exposed Ti^{n+} cations) on the TiO_2 surface.[16,17] It was demonstrated that the new-type of D–π–A dye sensitizers can inject electrons efficiently from the pyridyl group to the conduction band (CB) of the TiO_2 electrode through the coordinate bonding, rather than the bidentate bridging linkages of conventional D–π–A dye sensitizers bearing carboxyl group. Recently, Wang *et al.* reported that DSSCs based on D–π–A porphyrin dye bearing a pyridyl group reached solar energy-to-electricity conversion yield (η) of 3.96%.[18a] On the other hand, Goutsolelos *et al.* reported the η value of 3.9% for DSSC based on porphyrin dye bearing four pyridyl groups.[18c] However, the adsorption amounts ($<5.0 \times 10^{16}$ molecules per cm^2) of these porphyrin dye sensitizers bearing pyridyl group adsorbed on TiO_2 electrode are much lower than those of porphyrin dye sensitizers bearing carboxyl group, and thus the low dye loading leads to low light-harvesting efficiency (LHE) and poor surface coverage of the TiO_2 electrode, resulting in lowering of the photovoltaic performances of DSSCs.[18,19] More recently, Goutsolelos *et al.* have designed and synthesized "spider-shaped" porphyrin dye sensitizer bearing oligophenylenevinylene moieties, long dodecyloxy chains, and four pyridyl groups, which showed high dye loading value (1.9×10^{17} molecules per cm^2) due to an increase in the basicity of the pyridyl groups. As the results, the DSSC based on the "spider-shaped" porphyrin dye sensitizer reached the η value of 5.12%.[18e]

Recently, we have designed and prepared cyclic free-base porphyrin dimers (**H_4–C_4-CPD_{Py}(TEO)** and **H_4-Ptz-CPD_{Py}(TEO)**) linked by butadiyne or phenothiazine bearing four 4-pyridyl groups and their inclusion complexes (**$C_{60}\subset H_4$-C_4-CPD_{Py}(TEO)** and **$C_{60}\subset H_4$-Ptz-CPD_{Py}(TEO)**) with fullerene C_{60}.[20] It was found that these porphyrin dimers have favorable photochemical and electrochemical properties for DSSC through the electrochemical measurements and the transient absorption spectroscopy. Moreover, as for phenothiazine derivative **H_4-Ptz-CPD_{Py}(TEO)**, it would be expected that the phenothiazine unit possessing electron donating ability can provide a unidirectional flow of electrons toward the pyridyl anchoring group upon photoexcitation of the porphyrin, leading to the efficient electron injection from the photoexcited dye to the CB of TiO_2 electrode. Thus, in this work, to achieve high dye loading and high surface coverage of the TiO_2 electrode for DSSCs based on porphyrin dye sensitizers bearing pyridyl group, the cyclic free-base porphyrin dimers **H_4-C_4-CPD_{Py}(TEO)** and **H_4-Ptz-CPD_{Py}(TEO)** and their C_{60} inclusion complexes **$C_{60}\subset H_4$-C_4-CPD_{Py}(TEO)** and **$C_{60}\subset H_4$-Ptz-CPD_{Py}(TEO)** have been applied to DSSCs as a new class of porphyrin dye sensitizers bearing pyridyl anchoring groups for attachment on TiO_2 electrode (Scheme 1). It was demonstrated that these porphyrin dimers are adsorbed on the TiO_2 surface through the formations of hydrogen bonding of pyridyl groups and/or pyridinium ion at Brønsted acid sites on the TiO_2 surface. Here we reveal the photovoltaic performances of DSSCs based on these porphyrin dimers from kinetic and thermodynamic consideration concerning the electron transfer processes in DSSCs, based on the electrochemical measurements (voltammetry and electrochemical impedance spectroscopy) and the transient absorption spectroscopy.

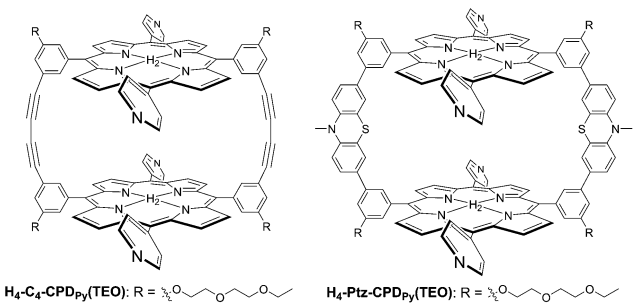

Scheme 1 Cyclic free-base porphyrin dimers (H_4-C_4-CPD_{Py}(TEO) and H_4-Ptz-CPD_{Py}(TEO)) bearing 4-pyridyl groups.

Results and discussion

Photoabsorption properties of cyclic free-base porphyrin dimers and their inclusion complexes with fullerene C_{60}

The synthesis of **H_4-Ptz-CPD_{Py}(TEO)** has been reported elsewhere.[20e] The synthetic pathway for **H_4-C_4-CPD_{Py}(TEO)** is shown in Scheme 2. The inclusion complexes **$C_{60}\subset H_4$-C_4-CPD_{Py}(TEO)** and **$C_{60}\subset H_4$-Ptz-CPD_{Py}(TEO)** with C_{60} were prepared by slowly evaporating the mixed solution of the corresponding cyclic free-base porphyrin dimer in chloroform (0.1 mM, 5 mL) and C_{60} in toluene (0.1 mM, 5 mL). The UV/vis absorption spectra of cyclic free-base porphyrin dimers **H_4-C_4-CPD_{Py}(TEO)** and **H_4-C_4-CPD_{Py}(TEO)** in benzonitrile are shown in Fig. 1 and their spectral data are summarized in Table 1. The porphyrin dimers **H_4-C_4-CPD_{Py}(TEO)** and **H_4-Ptz-CPD_{Py}(TEO)** exhibit strong Soret band at around 420 nm and relatively weak Q band in the range 500–650 nm. For the C_{60} inclusion complexes **$C_{60}\subset H_4$-C_4-CPD_{Py}(TEO)** and **$C_{60}\subset H_4$-Ptz-CPD_{Py}(TEO)**, it is difficult to

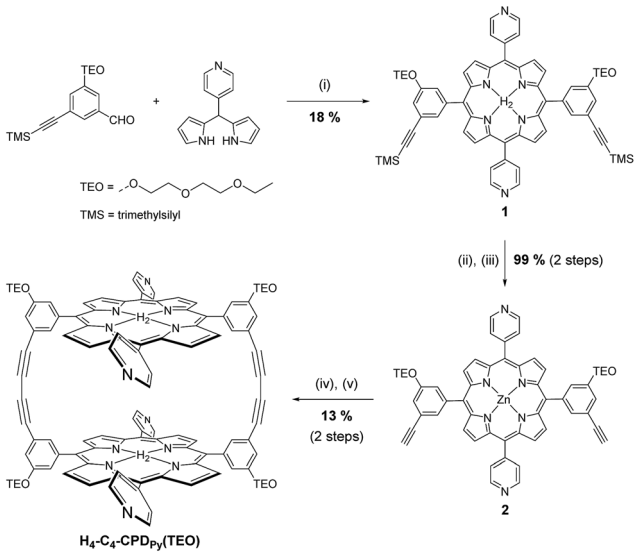

Scheme 2 Synthetic pathway for H_4-C_4-CPD_{Py}(TEO). (i) TFA, DDQ, CH_2Cl_2; (ii) $Zn(OAc)\cdot 2H_2O$, MeOH, CH_2Cl_2; (iii) KF, DMF; (iv) CuCl, pyridine, air; (v) HCl aq.

Open Access Article. Published on 02 February 2016. Downloaded on 12/4/2025 4:25:01 PM.
This article is licensed under a Creative Commons Attribution 3.0 Unported Licence.

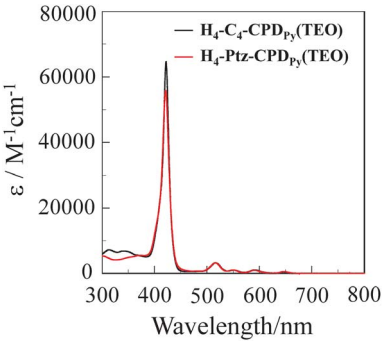

Fig. 1 UV/vis absorption spectra of H_4-C_4-CPD_{Py}(TEO) and H_4-Ptz-CPD_{Py}(TEO) in benzonitrile.

obtain their exact absorption spectra because the 1 : 1 complex of **H_4-C_4-CPD_{Py}(TEO)** or **H_4-Ptz-CPD_{Py}(TEO)** with C_{60} is in dissociation equilibrium in solution of 10^{-5} to 10^{-6} M concentration which is suitable for the measurement of absorption spectra of porphyrins. In our previous work, however, we have demonstrated that upon addition of C_{60} to the benzonitrile solution of the cyclic porphyrin dimers, their Soret bands were redshifted with a decrease in intensity, whereas their Q bands were slightly redshifted but increased in intensity.[20]

The UV/vis absorption spectra of cyclic free-base porphyrin dimers and their C_{60} inclusion complexes adsorbed on TiO_2 film are shown in Fig. 2. It is worth mentioning here that the adsorption amount of the porphyrin dimers adsorbed on TiO_2 film is 2.0×10^{17} molecules per cm^2, that is, the adsorption amount of porphyrin unit is 4.0×10^{17} cm^{-2}, which is higher than those ($<2.0 \times 10^{17}$ molecules per cm^2) of porphyrin dye sensitizers and D–π–A dye sensitizer bearing pyridyl groups reported so far.[16,18] The Soret bands of **C_{60}⊂H_4-C_4-CPD_{Py}(TEO)** and **C_{60}⊂H_4-Ptz-CPD_{Py}(TEO)** were redshifted compared to those of **H_4-C_4-CPD_{Py}(TEO)** and **H_4-Ptz-CPD_{Py}(TEO)**, although there is little difference in the Q band between the cyclic free-base porphyrin dimers and their C_{60} inclusion complexes. Thus, the UV/vis absorption spectra of these porphyrin dimers-adsorbed TiO_2 films are in good agreement with those in benzonitrile.

Electrochemical and photochemical properties of cyclic free-base porphyrin dimers and their inclusion complexes with fullerene C_{60}

The electrochemical properties of cyclic free-base porphyrin dimers and their C_{60} inclusion complexes were determined by cyclic voltammetry (CV) and differential pulse voltammetry (DPV) (see Fig. S7–S10 in ESI†).[20] The oxidation potential of the porphyrin unit in **C_{60}⊂H_4-C_4-CPD_{Py}(TEO)** (0.74 V *vs.* Fc/Fc^+) showed anodic shift by 0.03 V, compared with that of **H_4-C_4-CPD_{Py}(TEO)** (0.71 V) (Table 1). The oxidation potential of the porphyrin unit in **C_{60}⊂H_4-Ptz-CPD_{Py}(TEO)** (0.75 V) also showed anodic shift by 0.03 V, compared with that of **H_4-Ptz-CPD_{Py}(TEO)** (0.72 V). The reduction potentials corresponding to the reduction of the fullerene entity of **C_{60}⊂H_4-C_4-CPD_{Py}(TEO)** and **C_{60}⊂H_4-Ptz-CPD_{Py}(TEO)** were observed at −0.94 V and −0.96 V, respectively, which is cathodically shifted by 0.02 V and 0.04 V, respectively, compared to pristine C_{60} (−0.92 V).[20e] The small anodic shift of the oxidation potential of the porphyrin and the small cathodic shift of the reduction potential of C_{60} compared with their reference compounds is indicative of the charge transfer interaction between the porphyrins and C_{60}. The HOMO and LUMO energy levels were evaluated from the oxidation wave and the singlet excited energy of these porphyrin dimers (1.90 eV) based on the Q absorption band and fluorescence band in benzonitrile (*ca.* 650 nm), respectively. The HOMO and LUMO energy levels of these porphyrin dimers was *ca.* −5.5 eV and *ca.* −3.6 eV, respectively (Table 1). Thus, this result shows that the HOMO energy levels are more positive than the I_3^-/I^- redox potential (−4.9 eV), and thus this indicates that an efficient regeneration of the oxidized porphyrin dimers by electron transfer from the I_3^-/I^- redox couple in the electrolyte is thermodynamically feasible. Evidently, the LUMO energy levels of these porphyrin dimers are higher than the energy level (E_{cb}) of the CB of TiO_2 (−4.0 eV), suggesting that an electron injection to the CB of TiO_2 is thermodynamically feasible (some researchers have proposed that an energy gap of over 0.2–0.3 eV is necessary for efficient electron injection).[2–7]

Time-resolved absorption spectroscopy for cyclic free-base porphyrin dimers and their C_{60} inclusion complexes was performed by femtosecond laser flash photolysis after photoexcitation.[20] The photodynamics of these porphyrin dimers is summarized in Fig. 3. The decay of photoexcited state of **C_{60}⊂H_4-C_4-CPD_{Py}(TEO)** has two steps: the first step has a lifetime of 18 ps, which corresponds to the disappearance of the singlet excited state of the **$^1H_4$-C_4-CPD_{Py}(TEO)*** (*ca.* −3.6 eV), that is, the **$^1H_4$-C_4-CPD_{Py}(TEO)*** undergoes intrasupramolecular electron transfer to give a completely charge-separated state **$C_{60}^{\bullet-}$-H_4-C_4-CPD_{Py}(TEO)$^{\bullet+}$** (*ca.* −3.7 eV). The **$C_{60}^{\bullet-}$-H_4-C_4-CPD_{Py}(TEO)$^{\bullet+}$** decays with a lifetime of 470 ps to the ground state. The decay of photoexcited state of **C_{60}⊂H_4-Ptz-**

Table 1 Optical, electrochemical data and HOMO and LUMO energy levels of H_4-C_4-CPD_{Py}(TEO), C_{60}⊂H_4-C_4-CPD_{Py}(TEO), H_4-Ptz-CPD_{Py}(TEO), and C_{60}⊂H_4-Ptz-CPD_{Py}(TEO)

Porphyrin dimers	λ_{max}^{abs}/nm (ε/M^{-1} cm^{-1})[a]	E_{pa}^{ox}[b]/V *vs.* Fc/Fc^+	HOMO[c]/eV	LUMO[c]/eV
H_4-C_4-CPD_{Py}(TEO)	422 (646 000), 517 (30 800), 551 (9800), 590 (9600), 647 (4300)	0.71	−5.51	−3.61
C_{60}⊂H_4-C_4-CPD_{Py}(TEO)	—	0.74	−5.54	−3.64
H_4-Ptz-CPD_{Py}(TEO)	421 (55 800), 516 (32 100), 550 (10 500), 590 (9500), 646 (5600)	0.72	−5.52	−3.62
C_{60}⊂H_4-Ptz-CPD_{Py}(TEO)	—	0.75	−5.55	−3.65

[a] In benzonitrile. [b] Anodic (E_{pa}) peak potentials for oxidation were recorded in benzonitrile/Bu_4NPF_6 (0.1 M) solution for the porphyrin unit in **H_4-C_4-CPD_{Py}(TEO)**, **C_{60}⊂H_4-C_4-CPD_{Py}(TEO)**, **H_4-Ptz-CPD_{Py}(TEO)** and **C_{60}⊂H_4-Ptz-CPD_{Py}(TEO)**. [c] HOMO and LUMO energy levels of the porphyrin unit.

 This journal is © The Royal Society of Chemistry 2016

Open Access Article. Published on 02 February 2016. Downloaded on 12/4/2025 4:25:01 PM.
This article is licensed under a Creative Commons Attribution 3.0 Unported Licence.

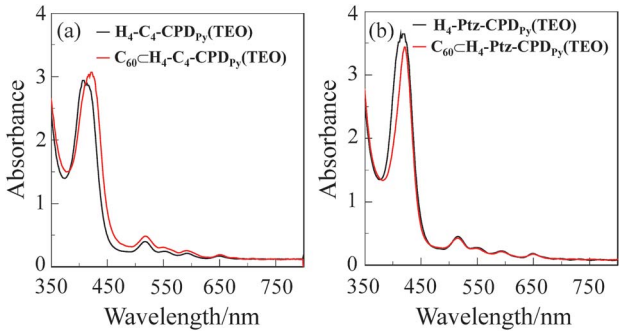

Fig. 2 UV/vis absorption spectra of (a) H_4-C_4-CPD_{Py}(TEO) and $C_{60}\subset H_4$-C_4-CPD_{Py}(TEO) and (b) H_4-Ptz-CPD_{Py}(TEO) and $C_{60}\subset H_4$-Ptz-CPD_{Py}(TEO) adsorbed on TiO_2 film (3 μm).

CPD_{Py}(TEO) also includes the charge-separated states **$C_{60}^{\bullet-}$-H_4-Ptz-CPD_{Py}(TEO)$^{\bullet+}$** (*ca.* −3.8 eV), but has multiple steps to the ground state *via* the triplet charge separated state **^{3}($C_{60}^{\bullet-}$-H_4-Ptz$^{\bullet+}$-CPD_{Py}(TEO))** (*ca.* −4.3 eV) with a lifetime of 0.71 ms: the first step has a lifetime of 20 ps, which is similar to that (18 ps) of **$C_{60}\subset H_4$-C_4-CPD_{Py}(TEO)**. On the other hand, the energy diagrams for the photochemical events in these porphyrin dimes revealed that the energy levels of charge-separated states is very close to or lower than the E_{cb} of the CB of TiO_2 electrode. This suggests that the electron injection from the **$C_{60}^{\bullet-}$** in the charge-separated states to the CB of TiO_2 electrode is thermodynamically difficult.

FTIR spectra of cyclic free-base porphyrin dimers and their inclusion complexes with fullerene C_{60}

To elucidate the adsorption states of cyclic free-base porphyrin dimers and their C_{60} inclusion complexes on TiO_2 nanoparticles, we measured the FTIR spectra of the porphyrin dimer powders and the porphyrin dimers adsorbed on TiO_2 nanoparticles (Fig. 4). For the powders of all the four porphyrin dimers **H_4-C_4-CPD_{Py}(TEO)**, **H_4-Ptz-CPD_{Py}(TEO)**, **$C_{60}\subset H_4$-C_4-CPD_{Py}(TEO)**, and **$C_{60}\subset H_4$-Ptz-CPD_{Py}(TEO)**, the C═N stretching band of pyridyl group was clearly observed at around 1590 cm^{-1}. Interestingly, when these porphyrin dimers were adsorbed on the TiO_2 surface, a new band appeared at around 1650 cm^{-1}, which indicates the formation of a pyridinium ion with Brønsted acid sites on TiO_2 surface.[21] In addition, the C═N

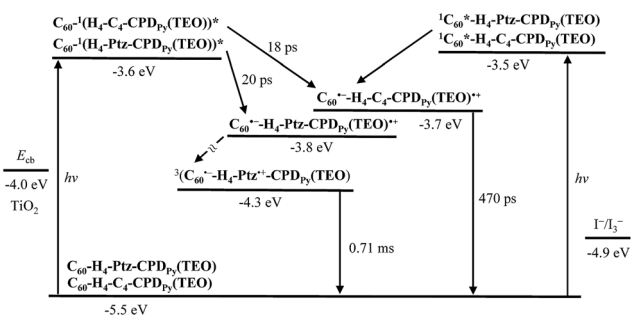

Fig. 3 Energy diagrams for the photochemical events in $C_{60}\subset H_4$-C_4-CPD_{Py}(TEO) and $C_{60}\subset H_4$-Ptz-CPD_{Py}(TEO).

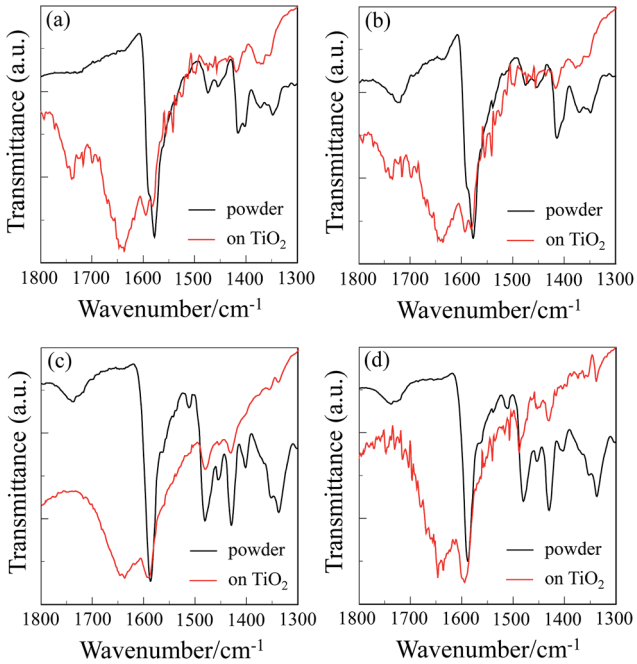

Fig. 4 FTIR spectra of the porphyrin dimer powders and the porphyrin dimers adsorbed on TiO_2 nanoparticles for (a) H_4-C_4-CPD_{Py}(TEO), (b) $C_{60}\subset H_4$-C_4-CPD_{Py}(TEO), (c) H_4-Ptz-CPD_{Py}(TEO), and (d) $C_{60}\subset H_4$-Ptz-CPD_{Py}(TEO).

stretching band at around 1590 cm^{-1} is shifted by 3–5 cm^{-1} to higher wavenumber, that is, the resulting band can be assigned to the hydrogen-bonded pyridyl group to Brønsted acid sites on the TiO_2 surface. Consequently, these observations demonstrate that these porphyrin dimers are adsorbed on the TiO_2 surface through the formations of hydrogen bonding of pyridyl groups and/or pyridinium ion at Brønsted acid sites on the TiO_2 surface. Thus, the UV/vis absorption and the FTIR spectra of the porphyrin dimers adsorbed on TiO_2 film indicate that high dye loading and high surface coverage of the TiO_2 electrode for DSSCs based on porphyrin dye sensitizers bearing pyridyl group are achieved by employing the cyclic porphyrin dimers bearing four pyridyl anchoring groups possessing the bonding ability to the two points on Brønsted acid sites on TiO_2 surface.

Photovoltaic performances of DSSCs based on cyclic free-base porphyrin dimers and their inclusion complexes with fullerene C_{60}

The DSSC was prepared using the dye-adsorbed TiO_2 electrode (9 μm), Pt-coated glass as a counter electrode, and an acetonitrile solution with iodine (0.05 M), lithium iodide (0.1 M), and 1,2-dimethyl-3-propylimidazolium iodide (0.6 M) as an electrolyte. The photocurrent–voltage (*I–V*) characteristics were measured under simulated solar light (AM 1.5, 100 mW cm^{-2}). The incident photon-to-current conversion efficiency (IPCE) spectra and the *I–V* curves are shown in Fig. 5. The photovoltaic performance parameters are collected in Table 2. The IPCE values corresponding to the Soret band (29% at 424 nm) and the Q band (6% at 520 nm) for the phenothiazine-bridged cyclic

Open Access Article. Published on 02 February 2016. Downloaded on 12/4/2025 4:25:01 PM.
This article is licensed under a Creative Commons Attribution 3.0 Unported Licence.

porphyrin dimer **H_4-Ptz-CPD_{Py}(TEO)** are higher than those (15% at 420 nm for the Soret band and 2% at 522 nm for the Q band) of the butadiyne-linked cyclic porphyrin dimer **H_4-C_4-CPD_{Py}(TEO)** (Fig. 5a). The *I–V* curves show that the short-circuit photocurrent density (J_{sc}) and η values of **H_4-Ptz-CPD_{Py}(TEO)** (1.40 mA cm^{-2} and 0.35%) are higher than those of **H_4–C_4-CPD_{Py}(TEO)** (0.79 mA cm^{-2} and 0.19%) (Fig. 5b). The higher photovoltaic performance for DSSC based on **H_4-Ptz-CPD_{Py}(TEO)** may be attributed to the efficient electron injection from the photoexcited dye (**$^1H_4$-Ptz-CPD_{Py}(TEO)***) to the CB of TiO_2 electrode because the phenothiazine unit possessing electron donating ability can provide a unidirectional flow of electrons toward the pyridyl anchoring group upon photoexcitation of the porphyrin. Interestingly, the photovoltaic performances of DSSC based on the C_{60} inclusion complexes **$C_{60}\subset H_4$-C_4-CPD_{Py}(TEO)** and **$C_{60}\subset H_4$-Ptz-CPD_{Py}(TEO)** are lower than those of **H_4-C_4-CPD_{Py}(TEO)** and **H_4-Ptz-CPD_{Py}(TEO)**. The electron injection (≈100 ps) from the photoexcited porphyrin to the CB of TiO_2 electrode is in kinetically competition with the intra-supramolecular electron transfer (18–20 ps), that is, the formation of charge-separated state **$C_{60}^{\bullet-}$-H_4-C_4-CPD_{Py}(TEO)$^{\bullet+}$** and **$C_{60}^{\bullet-}$-H_4-Ptz-CPD_{Py}(TEO)$^{\bullet+}$** (Fig. 3). Therefore, the lower photovoltaic performances for DSSC based on the C_{60} inclusion complexes would be attributed to the formation of charge-separated state, leading to low electron-injection efficiency from the photoexcited porphyrin to CB of TiO_2 electrode. On the other hand, the photovoltaic performance of DSSC based on **$C_{60}\subset H_4$-Ptz-CPD_{Py}(TEO)** is slightly lower than that of **$C_{60}\subset H_4$-C_4-CPD_{Py}(TEO)**, which may be attributed to the thermodynamically difficult electron-injection due to the lower triplet charge separated state **^{3}($C_{60}^{\bullet-}$-H_4-Ptz$^{\bullet+}$-CPD_{Py}(TEO))**.

Moreover, it is worth mentioning here that the open-circuit photovoltage (V_{oc}) values of the C_{60} inclusion complexes **$C_{60}\subset H_4$-C_4-CPD_{Py}(TEO)** (315 mV) and **$C_{60}\subset H_4$-Ptz-CPD_{Py}(TEO)** (304 mV) are lower than those of **H_4-C_4-CPD_{Py}(TEO)** (376 mV) and **H_4-Ptz-CPD_{Py}(TEO)** (396 mV). Thus, electrochemical impedance spectroscopy (EIS) analysis was performed to study the electron recombination process in DSSCs based on these porphyrin dimers in the dark under a forward bias of −0.60 V with a frequency range of 10 mHz to 100 kHz. The large semicircle in the Nyquist plot (Fig. 6a), which corresponds to the midfrequency peaks in the Bode phase plots, represents the charge recombination between the injected electrons in TiO_2 and I_3^- ions in the electrolyte, that is, the charge-transfer resistances at the TiO_2/dye/electrolyte interface. The Nyquist plots show that the resistance values of the large semicircle for **H_4-C_4-CPD_{Py}(TEO)** (13 Ω) and **H_4-Ptz-CPD_{Py}(TEO)** (14 Ω) are higher than those of **$C_{60}\subset H_4$-C_4-CPD_{Py}(TEO)** (5 Ω) and **$C_{60}\subset H_4$-Ptz-CPD_{Py}(TEO)** (5 Ω), indicating that the electron recombination resistances for **H_4-C_4-CPD_{Py}(TEO)** and **H_4-Ptz-CPD_{Py}(TEO)** are larger those of **$C_{60}\subset H_4$-C_4-CPD_{Py}(TEO)** and **$C_{60}\subset H_4$-Ptz-CPD_{Py}(TEO)**. The electron recombination lifetimes (τ_e) expressing the electron recombination between the injected electrons in TiO_2 and I_3^- ions in the electrolyte, extracted from the angular frequency (ω_{rec}) at the midfrequency peak in the Bode phase plot (Fig. 6b) using $\tau_e = 1/\omega_{rec}$, increase in the order of **$C_{60}\subset H_4$-C_4-CPD_{Py}(TEO)** (0.1 ms) and **$C_{60}\subset H_4$-Ptz-CPD_{Py}(TEO)** (0.1 ms) < **H_4-C_4-CPD_{Py}(TEO)** (2.2 ms) < **H_4-Ptz-CPD_{Py}(TEO)** (2.5 ms), respectively, which are consistent with the sequence of V_{oc} values in the DSSCs. Consequently, this is attributed to the fact that the formation of charge-separated state **$C_{60}^{\bullet-}$-H_4-C_4-CPD_{Py}(TEO)$^{\bullet+}$** and **$C_{60}^{\bullet-}$-H_4-Ptz-CPD_{Py}(TEO)$^{\bullet+}$** facilitates the approach of I_3^- ions to the TiO_2 surface because of complexation between the charge-separated state and I_3^-

Table 2 DSSC performance parameters of H_4-C_4-CPD_{Py}(TEO), $C_{60}\subset H_4$-C_4-CPD_{Py}(TEO), H_4-Ptz-CPD_{Py}(TEO), and $C_{60}\subset H_4$-Ptz-CPD_{Py}(TEO)

Porphyrin dimers[a]	J_{sc}/mA cm^{-2}[b]	V_{oc}[b]/mV	ff[b]	η[b] (%)
H_4-C_4-CPD_{Py}(TEO)	0.79	376	0.64	0.19
$C_{60}\subset H_4$-C_4-CPD_{Py}(TEO)	0.27	315	0.69	0.06
H_4-Ptz-CPD_{Py}(TEO)	1.40	396	0.63	0.35
$C_{60}\subset H_4$-Ptz-CPD_{Py}(TEO)	0.24	304	0.54	0.04

[a] The adsorption amount of the porphyrin dimers adsorbed on TiO_2 electrode is 2.0 × 10^{17} molecules per cm^2 under the adsorption condition of 0.1 mM porphyrin dimer solution in chloroform. The amount of adsorbed dye on TiO_2 electrode was determined form the calibration curve by absorption spectral measurement of the concentration change of the dye solution before and after adsorption. [b] Under a simulated solar light (AM 1.5, 100 mW cm^{-2}).

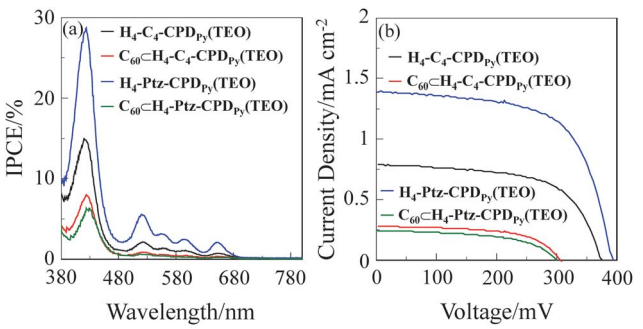

Fig. 5 (a) IPCE spectra and (b) *I–V* curves of DSSCs based on H_4-C_4-CPD_{Py}(TEO), $C_{60}\subset H_4$–C_4-CPD_{Py}(TEO), H_4-Ptz-CPD_{Py}(TEO), and $C_{60}\subset H_4$-Ptz-CPD_{Py}(TEO).

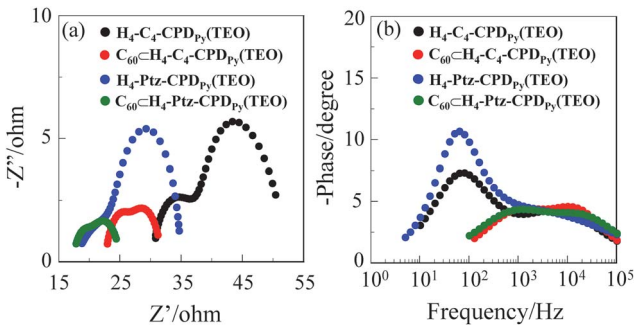

Fig. 6 (a) Nyquist plots and (b) Bode phase plots of DSSCs based on H_4-C_4-CPD_{Py}(TEO), $C_{60}\subset H_4$-C_4-CPD_{Py}(TEO), H_4-Ptz-CPD_{Py}(TEO), and $C_{60}\subset H_4$-Ptz-CPD_{Py}(TEO).

Open Access Article. Published on 02 February 2016. Downloaded on 12/4/2025 4:25:01 PM.
This article is licensed under a Creative Commons Attribution 3.0 Unported Licence.

ions, leading to faster charge recombination and thus resulting in a lower V_{oc} value.[3,6]

Conclusions

In this work, to seek a direction in molecular design toward creating a new class of porphyrin dye sensitizers bearing pyridyl anchoring groups for achieving high dye loading and high surface coverage of the TiO_2 electrode for dye-sensitized solar cells (DSSCs), cyclic free-base porphyrin dimers (**H_4-C_4-CPD_{Py}(TEO)** and **H_4-Ptz-CPD_{Py}(TEO)**) linked by butadiyne or phenothiazine bearing 4-pyridyl groups and their C_{60} inclusion complexes (**$C_{60}\subset H_4$-C_4-CPD_{Py}(TEO)** and **$C_{60}\subset H_4$-Ptz-CPD_{Py}(TEO)**) have been applied to DSSCs as the dye sensitizers. The Soret bands of **$C_{60}\subset H_4$-C_4-CPD_{Py}(TEO)** and **$C_{60}\subset H_4$-Ptz-CPD_{Py}(TEO)** were redshifted with a decrease in intensity, whereas their Q bands were slightly redshifted but increased in intensity, compared to **H_4-C_4-CPD_{Py}(TEO)** and **H_4-Ptz-CPD_{Py}(TEO)**. These porphyrin dimers are adsorbed on the TiO_2 surface through the formations of hydrogen bonding of pyridyl groups and/or pyridinium ion at Brønsted acid sites on the TiO_2 surface. It was found that the adsorption amount of the porphyrin dimers adsorbed on TiO_2 film is 2.0×10^{17} molecules per cm^2, that is, the adsorption amount of porphyrin unit is 4.0×10^{17} cm^{-2}, which is higher than those ($<2.0 \times 10^{17}$ molecules per cm^2) of porphyrin dye sensitizers and D–π–A dye sensitizer bearing pyridyl groups reported so far. The higher photovoltaic performance for DSSC based on **H_4-Ptz-CPD_{Py}(TEO)** relative to **H_4-C_4-CPD_{Py}(TEO)** may be attributed to the efficient electron injection from the photoexcited dye (**$^1H_4$-Ptz-CPD_{Py}(TEO)***) to the CB of TiO_2 because the phenothiazine unit possessing electron donating ability can provide a unidirectional flow of electrons toward the pyridyl anchoring group upon photoexcitation of the porphyrin. On the other hand, the photovoltaic performances of DSSC based on **$C_{60}\subset H_4$-C_4-CPD_{Py}(TEO)** and **$C_{60}\subset H_4$-Ptz-CPD_{Py}(TEO)** are lower than those of **H_4-C_4-CPD_{Py}(TEO)** and **H_4-Ptz-CPD_{Py}(TEO)**. The transient absorption spectroscopy and electrochemical measurements revealed that the lower photovoltaic performances for DSSC based on the C_{60} inclusion complexes would be attributed to the formation of charge-separated state between the photoexcited porphyrin and C_{60}, leading to low electron-injection efficiency from the photoexcited porphyrin to TiO_2 electrode. Consequently, this work provides that the cyclic porphyrin dimers with four pyridyl anchoring groups possessing bonding ability to the two points on Brønsted acid sites on TiO_2 surface, which can achieve the high dye loading and the high surface coverage of the TiO_2 electrode, would be expected to be one of the most promising classes of porphyrin dye sensitizers with pyridyl group.

Experimental

General

Infrared (IR) absorption spectra were recorded on a Perkin Elmer Spectrum One FT-IR spectrometer by ATR method and a Bio-Rad FTS6000 spectrometer by KBr disk method. Ultraviolet/visible (UV/vis) absorption spectra were observed with Shimadzu UV-3150 and UV-2500PC spectrophotometers. Nuclear magnetic resonance (NMR) spectra were recorded on a Bruker AVANCE III 600 spectrometer. The resonance frequencies are 600 MHz for ^1H and 151 MHz for ^{13}C. Chemical shifts were reported as δ values in ppm relative to tetramethylsilane. High-resolution fast atom bombardment mass spectra (HR-FAB-MS) were measured with 3-nitrobenzyl alcohol (NBA) as a matrix and recorded on a JEOL LMS-HX-110 spectrometer. Melting point (Mp) measurements were carried out on a Yanaco MP-S3 melting point meter. Cyclic voltammetry (CV) and differential pulse voltammetry (DPV) were carried out on an ALS630C (BAS, Japan) electrochemical analyzer in deaerated benzonitrile containing 0.1 M tetra-*n*-butylammonium hexafluorophosphate (Bu_4NPF_6) as a supporting electrolyte at room temperature under an Ar atmosphere. A conventional three-electrode cell was used with a platinum working electrode (surface area of 0.3 mm^2) and a platinum wire as a counter electrode. The measured potentials were recorded with respect to an $Ag/AgNO_3$ (0.01 M) reference electrode. All potentials (*vs.* Ag^+/Ag) were converted to values with respect to that of the Fc^+/Fc redox couple, which was measured under the same conditions. The highest occupied molecular orbital (HOMO) and lowest unoccupied molecular orbital (LUMO) energy levels of porphyrin dimers were evaluated from the spectral analyses and the DPV data. The HOMO energy level was evaluated from the oxidation wave for porphyrin dimers. The LUMO energy level was estimated from the singlet excited energy of these porphyrin dimers (1.90 eV) based on the Q absorption band nm and fluorescence band in benzonitrile.

Synthesis

5,15-Bis{3-[2-(2-ethoxyethoxy)ethoxy]-5-[(trimethylsilyl)ethynyl]-phenyl}-10,20-di{4-pyridyl}porphine (1). A solution of 3-[2-(2-ethoxyethoxy)ethoxy]-5-[(trimethylsilyl)ethynyl]benz-aldehyde[22] (4.63 g, 13.8 mmol) and *meso*-(4-pyridyl)-dipyrromethane[23] (3.08 g, 13.9 mmol) in CH_2Cl_2 (1.4 L) was degassed with a stream of N_2 for 30 min. To this solution, trifluoroacetic acid (TFA) (12.3 mL, 166 mmol) was added and stirred under a N_2 atmosphere. After 30 min, the resultant mixture was neutralized with NEt_3 (23 mL, 0.17 mol) and then 2,3-dichloro-5,6-dicyano-1,4-benzoquinone (DDQ) (4.7 g, 21 mmol) dissolved in benzene (250 mL) was added to the mixture. After an overnight stirring, the resultant mixture was purified by column chromatography (silica-gel, $CHCl_3$/EtOH = 50/1) then recrystallized from $CHCl_3$/*i*-PrOH to give **1** as a purple solid (1.27 g, 18%). ^1H NMR ($CDCl_3$, 600 MHz): δ −2.91 (br-s, 2H, –NH), 0.27 (s, 18H, $-Si(CH_3)_3$), 1.18 (t, J = 7.2 Hz, 6H, $-O(CH_2CH_2O)_2CH_2C\underline{H}_3$), 3.52 (q, J = 7.2 Hz, 4H, $-O(CH_2CH_2O)_2C\underline{H}_2CH_3$), 3.63 (dd, J = 4.8 and 6.0 Hz, 4H, $-O(CH_2)_2OCH_2C\underline{H}_2OC_2H_5$), 3.76 (t, J = 4.8 Hz, 4H, $-O(CH_2)_2OC\underline{H}_2CH_2OC_2H_5$), 3.96 (t, J = 4.8 Hz, 4H, $-OCH_2C\underline{H}_2O(CH_2)_2OC_2H_5$), 4.36 (t, J = 4.8 Hz, 4H, $-OC\underline{H}_2CH_2O(CH_2)OC_2H_5$), 7.47 (br-s, 2H, Ar–H), 7.75 (br-s, 2H, Ar–H), 7.93 (br-s, 2H. Ar–H), 8.17 (d, J = 5.4 Hz, 4H, Ar–H), 8.81 (d, J = 4.2 Hz, 4H, pyrrole β–H), 8.92 (d, J = 4.8 Hz, 4H, pyrrole β–H), 9.06 (d, J = 6.0 Hz, 4H, Ar–H); ^{13}C NMR ($CDCl_3$, 151 MHz): δ 0.1, 15.3, 66.9, 68.1, 69.9, 70.0, 71.2, 94.7, 104.9, 117.2, 117.4, 119.7, 122.6, 122.6, 129.6, 131.1,

Open Access Article. Published on 02 February 2016. Downloaded on 12/4/2025 4:25:01 PM. This article is licensed under a Creative Commons Attribution 3.0 Unported Licence.

143.1, 148.5, 150.3, 157.2; HR-FAB-MS (NBA): *m*/*z* calcd for $C_{64}H_{68}N_6O_6Si_2$: 1072.4739; found: 1072.4718; UV/vis ($CHCl_3$): λ_{max} (ε, cm^{-1} M^{-1}) 421 (392 000), 515 (18 200), 549 (5400), 588 (5400), 645 (2100); IR (KBr): ν = 3439, 3317, 3092, 3022, 2956, 2928, 2867, 2714, 2614, 2533, 2156, 1591, 1582, 1476, 1420, 1404, 352, 1323, 1297, 1247, 1196, 1173, 1161, 1114, 1069, 976, 927, 847, 800, 788, 760, 730, 697, 660, 563, 411 cm^{-1}; Mp: >300 °C.

{5,15-Di{3-[2-(2-ethoxyethoxy)ethoxy]-5-ethynyl]phenyl}-10,20-di{4-pyridyl}porphinato}zinc(II) (2). $Zn(OAc)_2 \cdot 2H_2O$ (2.4 g, 11 mmol) dissolved in MeOH (60 mL) was added to a solution of **1** (1.16 g, 1.08 mmol) in CH_2Cl_2 (1.1 L). The resultant mixture was refluxed overnight under N_2 atmosphere and then cooled to room temperature. The reaction mixture was neutralized with saturated aqueous solution of $NaHCO_3$ (200 mL), washed with water (200 mL, 2 times), dried over Na_2SO_4 and evaporated. The residue and $KF \cdot 2H_2O$ (0.63 g, 6.7 mmol) were dissolved in DMF (40 mL) and the mixture was stirred overnight under a N_2 atmosphere. After the stirring, the resultant mixture was diluted with $CHCl_3$ (100 mL) and washed with water (500 mL, 2 times). The organic layer was dried over Na_2SO_4 and evaporated to give the product as a purple solid (1.00 g, 99%). ^{1}H NMR (pyridine-d_5, 600 MHz): δ 1.00 (t, J = 7.2 Hz, 6H, $-O(CH_2CH_2O)_2CH_2C\underline{H}_3$), 3.33 (q, J = 6.6 Hz, 4H, $-O(CH_2CH_2O)_2C\underline{H}_2CH_3$), 3.52 (t, J = 4.8 Hz, 4H, $-O(CH_2)_2OCH_2C\underline{H}_2OC_2H_5$), 3.67 (t, J = 4.8 Hz, 4H, $-O(CH_2)_2OC\underline{H}_2CH_2OC_2H_5$), 3.87 (t, J = 4.8 Hz, 4H, $-OCH_2C\underline{H}_2$-$O(CH_2)_2OC_2H_5$), 4.15 (s, 2H, –C≡CH) 4.31 (t, J = 4.8 Hz, 4H, $-OC\underline{H}_2CH_2O(CH_2)OC_2H_5$), 7.68 (d, J = 0.6 Hz, 2H, Ar–H), 8.05 (br-s, 2H, Ar–H), 8.23 (d, J = 4.2 Hz, 2H, Ar–H), 8.26 (d, J = 4.2 Hz, 4H, Ar–H), 9.02 (d, J = 4.8 Hz, 4H, pyrrole β–H), 9.11 (d, J = 5.4 Hz, 4H, Ar–H), 9.15 (d, J = 4.8 Hz, 4H, pyrrole β–H); ^{13}C NMR (pyridine-d_5, 151 MHz): δ 15.5, 66.5, 68.5, 70.0, 70.3, 71.2, 79.6, 84.5, 117.6, 118.7, 120.6, 122.0, 130.1, 131.7, 132.2, 132.9, 145.2, 148.7, 149.8, 150.3, 150.7, 151.4, 157.7; HR-FAB-MS (NBA): *m*/*z* calcd for $C_{58}H_{50}N_6O_6Zn$: 990.3083; found: 990.3082; UV/vis ($CHCl_3$): λ_{max} (ε, cm^{-1} M^{-1}) 425 (418 000), 555 (16 200), 595 (2400); IR (KBr): ν = 3433, 3283, 2972, 2928, 2872, 1592, 1581, 1540, 1523, 1488, 1456, 1419, 1344, 1321, 1298, 1283, 1246, 1204, 1181, 1113, 1071, 1048, 998, 938, 874, 819, 796, 763, 719, 675, 665, 569, 545, 436, 419 cm^{-1}; Mp: >300 °C.

H_4-C_4-CPD_{Py}(TEO). The free-base dimer was prepared from **2** (397 mg, 0.4 mmol) with CuCl (8.0 g, 80 mmol) in pyridine (1.2 L) according to the reported procedure.[20a,d] The crude product was purified by flash column chromatography (silica-gel, $CHCl_3$/EtOH = 100/1 to 10/1) and recrystallized from $CHCl_3$/*i*-PrOH to give the product as a purple powder (48 mg, 13%). ^{1}H NMR ($CDCl_3$, 600 MHz): δ −3.04 (br-s, 4H, –NH), 1.21 (t, J = 7.2 Hz, 12H, $-O(CH_2CH_2O)_2CH_2C\underline{H}_3$), 3.55 (q, J = 7.2 Hz, 8H, $-O(CH_2CH_2O)_2C\underline{H}_2CH_3$), 3.67 (dd, J = 4.8 and 6.0 Hz, 8H, $-O(CH_2)_2OCH_2C\underline{H}_2OC_2H_5$), 3.81 (dd, J = 4.8 and 6.0 Hz, 8H, $-O(CH_2)_2OC\underline{H}_2CH_2OC_2H_5$), 4.03 (t, J = 4.8 Hz, 8H, $-OCH_2C\underline{H}_2$-$O(CH_2)_2OC_2H_5$), 4.42 (t, J = 4.8 Hz, 8H, $-OC\underline{H}_2CH_2O(CH_2)OC_2H_5$), 6.88 (s, 4H, Ar–H), 7.25 (dd, J = 0.6 and 1.8 Hz, 4H, Ar–H), 7.94 (br-s, 8H, Ar–H), 8.22 (t, J = 1.8 Hz, 4H, Ar–H), 8.62 (d, J = 4.2 Hz, 8H, pyrrole β–H), 8.70 (d, J = 4.2 Hz, 8H, pyrrole β–H), 8.96 (br-s, 8H, Ar–H); ^{13}C NMR ($CDCl_3$, 151 MHz): δ 15.3, 66.9, 68.3, 70.0, 70.1, 71.3, 74.5, 83.1, 114.9, 117.1, 118.6, 120.4, 120.8, 129.3, 135.3, 143.0, 148.4, 149.9, 157.8; HR-FAB-MS (NBA): *m*/*z* calcd for $C_{116}H_{100}N_{12}O_{12}$: 1852.7584; found: 1852.7545; UV/vis (PhCN): λ_{max} (ε, cm^{-1} M^{-1}); 422 (646 000), 517 (30 800), 551 (9800), 590 (9600), 647 (4300); IR (ATR): ν = 3312, 2971, 2920, 2865, 1578, 1474, 1455, 1415, 1372, 1348, 1285, 1254, 1221, 1195, 1172, 1108, 1062, 993, 974, 930, 871, 849, 797, 728, 692, 659, 563, 540, 517, 467, 411 cm^{-1}; Mp: >300 °C.

Preparation of DSSCs

The TiO_2 paste (JGC Catalysts and Chemicals Ltd., PST-18NR) was deposited on a fluorine-doped-tin-oxide (FTO) substrate by doctor-blading, and sintered for 50 min at 450 °C. The 9 μm thick TiO_2 electrode was immersed into 0.1 mM porphyrin dimer solution in chloroform for 15 hours enough to adsorb the dye sensitizers. The DSSCs were fabricated by using the TiO_2 electrode (0.5 × 0.5 cm^2 in photoactive area) thus prepared, Pt-coated glass as a counter electrode, and a solution of 0.05 M iodine, 0.1 M lithium iodide, and 0.6 M 1,2-dimethyl-3-propylimidazolium iodide in acetonitrile as electrolyte. The photocurrent–voltage characteristics were measured using a potentiostat under a simulated solar light (AM 1.5, 100 mW cm^{-2}). IPCE spectra were measured under monochromatic irradiation with a tungsten-halogen lamp and a monochromator. The amount of adsorbed dye on TiO_2 nanoparticles was determined form the calibration curve by absorption spectral measurement of the concentration change of the porphyrin dye solution before and after adsorption. Absorption spectra of the dyes adsorbed on TiO_2 nanoparticles were recorded on the porphyrin dyes-adsorbed TiO_2 film (thickness of 3 μm) in the transmission mode with a calibrated integrating sphere system. Electrochemical impedance spectroscopy (EIS) for DSSCs in the dark under a forward bias of −0.60 V with a frequency range of 10 mHz to 100 kHz was measured with a AMETEK Versa STAT 3.

Acknowledgements

This work was supported by Grants-in-Aid (No. 20108009 and 15K05432 to F. T. and No. 15H03859 to Y. O.) from Ministry of Education, Culture, Sports, Science and Technology of Japan and Research Grants to F. T. from Tokuyama Science and Technology Foundation and Iketani Science and Technology Foundation.

Notes and references

1 B. O'Regan and M. Grätzel, *Nature*, 1991, **353**, 737.
2 A. Hagfeldt, G. Boschloo, L. Sun, L. Kloo and H. Pettersson, *Chem. Rev.*, 2010, **110**, 6595.
3 (*a*) Z. Ning and H. Tian, *Chem. Commun.*, 2009, 5483; (*b*) Z. Ning, Y. Fu and H. Tian, *Energy Environ. Sci.*, 2010, **3**, 1170.
4 A. Mishra, M. K. R. Fischer and P. Bäuerle, *Angew. Chem., Int. Ed.*, 2009, **48**, 2474.
5 Y. Ooyama and Y. Harima, *Eur. J. Org. Chem.*, 2009, **18**, 2903.
6 Y. Ooyama and Y. Harima, *ChemPhysChem*, 2012, **13**, 4032.
7 N. Manfredi, B. Cecconi and A. Abbotto, *Eur. J. Org. Chem.*, 2014, 7069.

Open Access Article. Published on 02 February 2016. Downloaded on 12/4/2025 4:25:01 PM.
This article is licensed under a Creative Commons Attribution 3.0 Unported Licence.

8 (*a*) X. Wang, J. Yang, H. Yu, F. Li, L. Fan, W. Sun, Y. Liu, Z. Y. Koh, J. Pan, W.-L. Yim, L. Yan and Q. Wang, *Chem. Commun.*, 2014, **50**, 3965; (*b*) S.-G. Li, K.-J. Jiang, J.-H. Huang, L.-M. Yang and Y.-L. Song, *Chem. Commun.*, 2014, **50**, 4309; (*c*) D. K. Panda, F. S. Goodson, S. Ray and S. Saha, *Chem. Commun.*, 2014, **50**, 5358; (*d*) K. Kakiage, Y. Aoyama, T. Yano, T. Otsuka, T. Kyomen, M. Unno and M. Hanaya, *Chem. Commun.*, 2014, **50**, 6379; (*e*) A. Amacher, C. Yi, J. yang, M. P. Bircher, Y. Fu, M. Cascella, M. Grätzel, S. Decurtins and S.-X. Liu, *Chem. Commun.*, 2014, **50**, 6540; (*f*) J. Yang, P. Ganesan, J. Teuscher, T. Moehl, Y. J. Kim, C. Yi, P. Comte, K. Pei, T. W. Holcombe, M. K. Nazeeruddin, J. Hua, S. K. Zakeeruddin, H. Tian and M. Grätzel, *J. Am. Chem. Soc.*, 2014, **136**, 5772.

9 (*a*) T. Ikeuchi, H. Nomoto, N. Masaki, M. J. Griffith, S. Mori and M. Kimura, *Chem. Commun.*, 2014, **50**, 1941; (*b*) R. Agosta, R. Grisorio, L. De Marco, G. Romanazzi, G. P. Suranna, G. Gigli and M. Manca, *Chem. Commun.*, 2014, **50**, 9451; (*c*) A. Dessi, M. Calamante, A. Mordini, M. Peruzzin, A. Sinicropi, R. Basosi, F. F. de Biani, M. Taddei, D. Colonna, A. D. Carlo, G. Reginato and L. Zani, *Chem. Commun.*, 2014, **50**, 13952; (*d*) X. Sun, Y. Wang, X. Li, H. Ågren, W. Zhu, H. Tian and Y. Xie, *Chem. Commun.*, 2014, **50**, 15609.

10 (*a*) H. Imahori, T. Umeyama and S. Ito, *Acc. Chem. Res.*, 2009, **42**, 1809; (*b*) S. Eu, S. Hayashi, T. Umeyama, Y. Matano, Y. Araki and H. Imahori, *J. Phys. Chem. C*, 2008, **112**, 4396; (*c*) A. Kira, Y. Matsubara, H. Iijima, T. Umeyama, Y. Matano, S. Ito, M. Niemi, N. V. Tkachenko, H. Lemmetyinen and H. Imahori, *J. Phys. Chem. C*, 2010, **114**, 11293; (*d*) H. Imahori, H. Iijima, H. Hayashi, Y. Toude, T. Umeyama, Y. Matano and S. Ito, *ChemSusChem*, 2011, **4**, 797; (*e*) K. Kurotobi, Y. Toude, K. Kawamoto, Y. Fujimori, S. Ito, P. Chabera, V. Sundström and H. Imahori, *Chem.–Eur. J.*, 2013, **19**, 17075; (*f*) T. Higashino and H. Imahori, *Dalton Trans.*, 2015, **44**, 448.

11 (*a*) T. Bessho, S. M. Zakeeruddin, C.-Y. Yeh, E. W.-G. Diau and M. Grätzel, *Angew. Chem., Int. Ed.*, 2010, **49**, 6646; (*b*) A. Yella, H.-W. Lee, H. N. Tsao, C. Yi, A. K. Chandiran, M. K. Nazeeruddin, E. W.-G. Diau, C.-Y. Yeh, S. M. Zakeeruddin and M. Grätzel, *Science*, 2011, **334**, 629; (*c*) L.-L. Li and E. W.-G. Diau, *Chem. Soc. Rev.*, 2013, **42**, 291; (*d*) S. Mathew, A. Yella, P. Gao, R. Humphry-Baker, B. F. E. Curchod, N. Ashari-Astani, I. Tavernelli, U. Rothlisberger, M. K. Nazeeruddin and M. Grätzel, *Nat. Chem.*, 2014, **6**, 242; (*e*) A. Yella, C.-L. Mai, S. M. Zakeeruddin, S.-N. Chang, C.-H. Hsieh, C.-Y. Yeh and M. Grätzel, *Angew. Chem., Int. Ed.*, 2014, **53**, 2973.

12 (*a*) M. V. Martínez-Díaz, G. de la Torre and T. Torres, *Chem. Commun.*, 2010, **46**, 7090; (*b*) M. J. Griffith, K. Sunahara, P. Wagner, K. Wagner, G. G. Wallace, D. L. Officer, A. Furube, R. Katoh, S. Mori and A. J. Mozer, *Chem. Commun.*, 2012, **48**, 4145; (*c*) K. Ladomenou, T. N. Kitsopoulos, G. D. Sharma and A. G. Coutsolelos, *RSC Adv.*, 2014, **4**, 21379.

13 (*a*) Y.-C. Chang, C.-L. Wang, T.-Y. Pan, S.-H. Hong, C.-M. Lan, H.-H. Kuo, C.-F. Lo, H.-Y. Hsu, C.-Y. Lin and E. W.-G. Diau, *Chem. Commun.*, 2011, **47**, 8910; (*b*) M. Ishida, D. Hwang, Y. B. Koo, J. Sung, D. Y. Kim, J. L. Sessler and D. Kim, *Chem. Commun.*, 2013, **49**, 9164; (*c*) C. Lo, S. Hsu, C. Wang, Y. Cheng, H. Lu, E. W. Diau and C. Lin, *J. Phys. Chem. C*, 2010, **114**, 12018; (*d*) J. Lu, X. Xu, K. Cao, J. Cui, Y. Zhang, Y. Shen, X. Shi, L. Liao, Y. Cheng and M. Wang, *J. Mater. Chem. A*, 2013, **1**, 10008; (*e*) R. B. Ambre, G.-F. Chang, M. R. Zanwar, C.-F. Yao, E. W.-G. Diau and C.-H. Hung, *Chem.–Asian J.*, 2013, **8**, 2144; (*f*) R. B. Ambre, G.-F. Chang and C.-H. Hung, *Chem. Commun.*, 2014, **50**, 725.

14 (*a*) C.-L. Wang, Y.-C. Chang, C.-M. Lan, C.-F. Lo, E. Wei-Guang Diau and C.-Y. Lin, *Energy Environ. Sci.*, 2011, **4**, 1788; (*b*) C.-H. Wu, T.-Y. Pan, S.-H. Hong, C.-L. Wang, H.-H. Kuo, Y.-Y. Chu, E. W.-G. Diau and C.-Y. Lin, *Chem. Commun.*, 2012, **48**, 4329; (*c*) H.-P. Lu, C.-L. Mai, C.-Y. Tsia, S.-J. Hsu, C.-P. Hsieh, C.-L. Chiu, C.-Y. Yeh and E. W.-G. Diau, *Phys. Chem. Chem. Phys.*, 2009, **11**, 10270; (*d*) C.-H. Wu, M.-C. Chen, P.-C. Su, H.-H. Kuo, C.-L. Wang, C.-Y. Lu, C.-H. Tsai, C.-C. Wu and C.-Y. Lin, *J. Mater. Chem. A*, 2014, **2**, 991; (*e*) J. M. Ball, N. K. S. Davis, J. D. Wilkinson, J. Kirkpatrick, J. Teuscher, R. Gunning, H. L. Anderson and H. J. Snaith, *RSC Adv.*, 2012, **2**, 6846; (*f*) C.-L. Mai, W.-K. Huang, H.-P. Lu, C.-W. Lee, C.-L. Chiu, Y.-R. Liang, E. W.-G. Diau and C.-Y. Yeh, *Chem. Commun.*, 2010, **46**, 809.

15 (*a*) K. Sunahara, M. J. Griffith, T. Uchiyama, P. Wagner, D. L. Officer, G. G. Wallace, A. J. Mozer and S. Mori, *ACS Appl. Mater. Interfaces*, 2013, **5**, 10824; (*b*) T. Hamamura, J. T. Dy, K. Tamaki, J. Nakazaki, S. Uchida, T. Kubo and H. Segawa, *Phys. Chem. Chem. Phys.*, 2014, **16**, 4551; (*c*) H.-P. Wu, Z.-W. Ou, T.-Y. Pan, C.-M. Lan, W.-K. Huang, H.-W. Lee, N. M. Reddy, C.-T. Chen, W.-S. Chao, C.-Y. Yeh and E. W.-G. Diau, *Energy Environ. Sci.*, 2012, **5**, 9843; (*d*) C.-L. Wang, J.-Y. Hu, C.-H. Wu, H.-H. Kuo, Y.-C. Chang, Z.-J. Lan, H.-P. Wu, E. Wei-Guang Diau and C.-Y. Lin, *Energy Environ. Sci.*, 2014, **7**, 1392; (*e*) J. Luo, M. Xu, R. Li, K.-W. Huang, C. Jiang, Q. Qi, W. Zeng, J. Zhang, C. Chi, P. Wang and J. Wu, *J. Am. Chem. Soc.*, 2014, **136**, 265.

16 (*a*) Y. Ooyama, S. Inoue, R. Asada, G. Ito, K. Kushimoto, K. Komaguchi, I. Imae and Y. Harima, *Eur. J. Org. Chem.*, 2010, 92; (*b*) Y. Ooyama, S. Inoue, T. Nagano, K. Kushimoto, J. Ohshita, I. Imae, K. Komaguchi and Y. Harima, *Angew. Chem., Int. Ed.*, 2011, **50**, 7429; (*c*) Y. Ooyama, T. Nagano, S. Inoue, I. Imae, K. Komaguchi, J. Ohshita and Y. Harima, *Chem.–Eur. J.*, 2011, **17**, 14837; (*d*) Y. Ooyama, N. Yamaguchi, I. Imae, K. Komaguchi, J. Ohshita and Y. Harima, *Chem. Commun.*, 2013, **49**, 2548; (*e*) Y. Ooyama, Y. Hagiwara, T. Mizumo, Y. Harima and J. Ohshita, *New J. Chem.*, 2013, **37**, 2479; (*f*) Y. Ooyama, T. Sato, Y. Harima and J. Ohshita, *J. Mater. Chem. A*, 2014, **2**, 3293.

17 (*a*) Y. Harima, T. Fujita, Y. Kano, I. Imae, K. Komaguchi, Y. Ooyama and J. Ohshita, *J. Phys. Chem. C*, 2013, **117**, 16364; (*b*) N. Shibayama, H. Ozawa, M. Abe, Y. Ooyama and H. Arakawa, *Chem. Commun.*, 2014, **50**, 6398.

Open Access Article. Published on 02 February 2016. Downloaded on 12/4/2025 4:25:01 PM.
This article is licensed under a Creative Commons Attribution 3.0 Unported Licence.

18 (*a*) J. Lu, X. Xu, Z. Li, k. Cao, J. Cui, Y. Zhang, Y. Shen, Y. Li, J. Zhu, S. Dai, W. Chjen, Y. Cheng and M. Wang, *Chem.–Asian J.*, 2013, **8**, 956; (*b*) T. Sakurada, Y. Arai and H. Segawa, *RSC Adv.*, 2014, **4**, 13201; (*c*) D. Daphnomili, G. Landrou, P. Singh, A. Thomas, K. Yesudas, B. K. G. D. Sharma and A. G. Goutsolelos, *RSC Adv.*, 2012, **2**, 12899; (*d*) D. Daphnomili, G. D. Sharma, S. Biswas, T. K. R. Justin and A. G. Goutsolelos, *J. Photochem. Photobiol., A*, 2013, **253**, 88; (*e*) C. Stangel, A. Bagaki, P. A. Angaridis, G. Charalambidis, G. D. Sharma and A. G. Coutsolelos, *Inorg. Chem.*, 2014, **53**, 11871.

19 (*a*) M.-D. Zhang, H.-X. Xie, X.-H. Ju, L. Qin, Q.-X. Yang, H.-G. Zheng and X.-F. Zhou, *Phys. Chem. Chem. Phys.*, 2013, **15**, 634; (*b*) L. Wang, X. yang, S. Li, M. Cheng and L. Sun, *RSC Adv.*, 2013, **3**, 13677; (*c*) J. Mao, D. Wang, S.-H. Liu, Y. Hang, Y. Xu, Q. Zhang, W. Wu, P.-T. Chou and J. Hua, *Asian J. Org. Chem.*, 2014, **3**, 153; (*d*) J. Massin, L. Ducasse, T. Toupance and C. Olivier, *J. Phys. Chem. C*, 2014, **118**, 10677; (*e*) L. Zhang, J. M. Cole and C. Dai, *ACS Appl. Mater. Interfaces*, 2014, **6**, 7535.

20 (*a*) H. Nobukuni, Y. Shimazaki, H. Uno, Y. Naruta, K. Okubo, T. Kojima, S. Fukuzumi, S. Seki, H. Sakai, T. Hasobe and F. Tani, *Chem.–Eur. J.*, 2010, **16**, 11611; (*b*) H. Nobukuni, T. Kamimura, H. Uno, Y. Shimazaki, Y. Naruta and F. Tani, *Bull. Chem. Soc. Jpn.*, 2012, **85**, 862; (*c*) K. Sakaguchi, T. Kamimura, H. Uno, S. Mori, S. Ozako, H. Nobukuni, M. Ishida and F. Tani, *J. Org. Chem.*, 2014, **79**, 2980; (*d*) T. Kamimura, K. Ohkubo, Y. Kawashima, H. Nobukuni, Y. Naruta, F. Tani and S. Fukuzumi, *Chem. Sci.*, 2013, **4**, 1451; (*e*) T. Kamimura, K. Ohkubo, Y. Kawashima, S. Ozako, K. Sakaguchi, S. Fukuzumi and F. Tani, *J. Phys. Chem. C*, 2015, **119**, 25634.

21 (*a*) T. J. Dines, L. D. MacGregor and C. H. Rochester, *Phys. Chem. Chem. Phys.*, 2001, **3**, 2676; (*b*) M. I. Zaki, M. A. Hasan, F. A. Al-Sagheer and L. Pasupulety, *Colloids Surf., A*, 2001, **190**, 261; (*c*) O. Kasende and T. Zeegers-Huyskens, *J. Phys. Chem.*, 1984, **88**, 2132; (*d*) H. Takahashi, K. Mamola and E. K. Plyler, *J. Mol. Spectrosc.*, 1966, **21**, 217; (*e*) M. A. Montańez, I. L. Tocón, J. C. Otero and J. I. Marcos, *J. Mol. Struct.*, 1999, **482–483**, 201.

22 T. Kamimura, M. Komura, H. Komiyama, T. Iyoda and F. Tani, *Chem. Commun.*, 2015, **51**, 1685.

23 C. Ruzié, L. Michaudet and B. Boitrel, *Tetrahedron Lett.*, 2002, **43**, 7423.

 This journal is © The Royal Society of Chemistry 2016